

DETERMINATION OF DIFFERENTIAL LOCATIONS AND FOCAL MECHANISM OF THE 2013–2015. EARTHQUAKES IN TROSNYK, TRANSCARPATIANS: METHODOLOGICAL ASPECTS AND ANALYSIS OF THE RESULTS

The differential and source terms locations of a series of small ($1.0 < M_L < 2.5$) similar (recurrent) earthquakes that occurred during 2013–2015 near the village of Trosnyk in the south of Transcarpathians were determined. Adaptive filtering was proposed to reduce the effect of correlated noise in records with very low signal-to-noise ratio and to improve the reliability of differential arrivals. The maximum correlation criterion was modified to include the minimum departure from the calculated arrival times. Analysis of the intervals between phase arrivals at pairs of stations was proposed to further reduce the number of problematic arrivals. The sensitivity of the final solution to the network configuration was assessed using the *jack-knife* principle, when the coordinates are calculated, each time removing one station from the full set. The focal mechanism common to all earthquakes in the series was defined using the polarities of *P*-wave arrivals at 16 stations. Based on the results of the 3D interpretation of the differential hypocenters, the nodal plane with a strike of $\sim 150^\circ$ was identified as the rupture plane, and the mechanism itself was classified as left-lateral slip with a component of thrust. The epicenter of the strongest earthquake was located almost exactly on the fault of the pre-Neogene basement with a strike parallel to the Carpathian arc, almost the same as the strike of the rupture plane. The axis of compression in the focal mechanism is directed to the east, which is fully consistent with the northeast direction of the general regional field.

Key words: recurrent (similar) earthquakes; waveform correlation; differential arrivals; station terms; focal mechanism; fault-block tectonics; tectonic stress.

Introduction

The series of approximately 17 earthquakes had occurred during 2013–2015 approximately 10 km from the village of Trosnyk in the south of Transcarpathians (Fig. 1, Table 1). It can be considered typical for the region, both in terms of magnitude ($1.0 < M_L < 2.5$) and duration (at least for the western part of the region, where it is usually much longer than in the eastern one).

Improving the accuracy of the earthquake location is important in many problems of seismological research. They include determining the magnitude, focal mechanism, velocities and absorption coefficients of seismic waves, seismic hazard and risk, studying the internal structure of the Earth, fault-block tectonics and tectonic regime, especially in regions with a low level of seismicity, such as Ukrainian Transcarpathians, etc.

For this purpose, the correlation of waveforms of recurrent (or similar) earthquakes, which usually belong to swarms (series, clusters), foreshock or aftershock sequences, has been used more and more effectively in the recent decades [Shearer, 1997; Shearer et al., 2005; Waldhauser et al., 2000]. However, this applies not only to the estimation of the so-called differential arrivals by taking into

account the shifts of the maximum correlation between records, but also to the use of maximum values of correlation as a measure of the distance between foci. It enables to estimate relative (mutual) locations even from records of only one station [Robinson, et al., 2007, 2007, 2013; Gnyp, 2013, 2014; Harris & Douglas, 2021].

Recurrent earthquakes were also used to solve a variety of other seismological problems, including inferring the fault slip rates at depth [Nadeau & McEvelly, 1999], determining the lower mantle heterogeneity [Tibuleac & Herrin, 1999], monitoring velocity variations in the crust [Poupinet et al., 1984], identification of blasts [Verbytskyi et al., 2011; Harris, 1991] etc.

In Transcarpathians, the differential locations were previously determined simultaneously with source-specific station terms for the 2005–2006 series of earthquakes near Mukacheve [Gnyp, 2010] and 2015 near Teresva [Gnyp & Malyskyy, 2021]. The relative locations of the Mukacheve earthquakes were also estimated from the cross-correlation maxima between records compared to the bulletin, but also the shape and spatial orientation of the hypocenter cloud was established. Combined with the determination of the focal mechanism for the strongest earthquake, this

made it possible to identify the common rupture plane to which the other earthquakes belonged.

In these works, new methodological approaches were also proposed to both quality control of raw data and their direct interpretation. In particular, a significant time drift (sometimes even amounting to 1 s) at some seismic stations of the Carpathian network

was found by constructing diagrams of the intervals between P -wave arrivals of the same earthquakes at different stations. Also, the diagrams proved their usefulness in detecting erroneous arrivals, as well as interpreting the character of the spatial arrangement of earthquakes, which is especially important during the identification of the rupture plane.

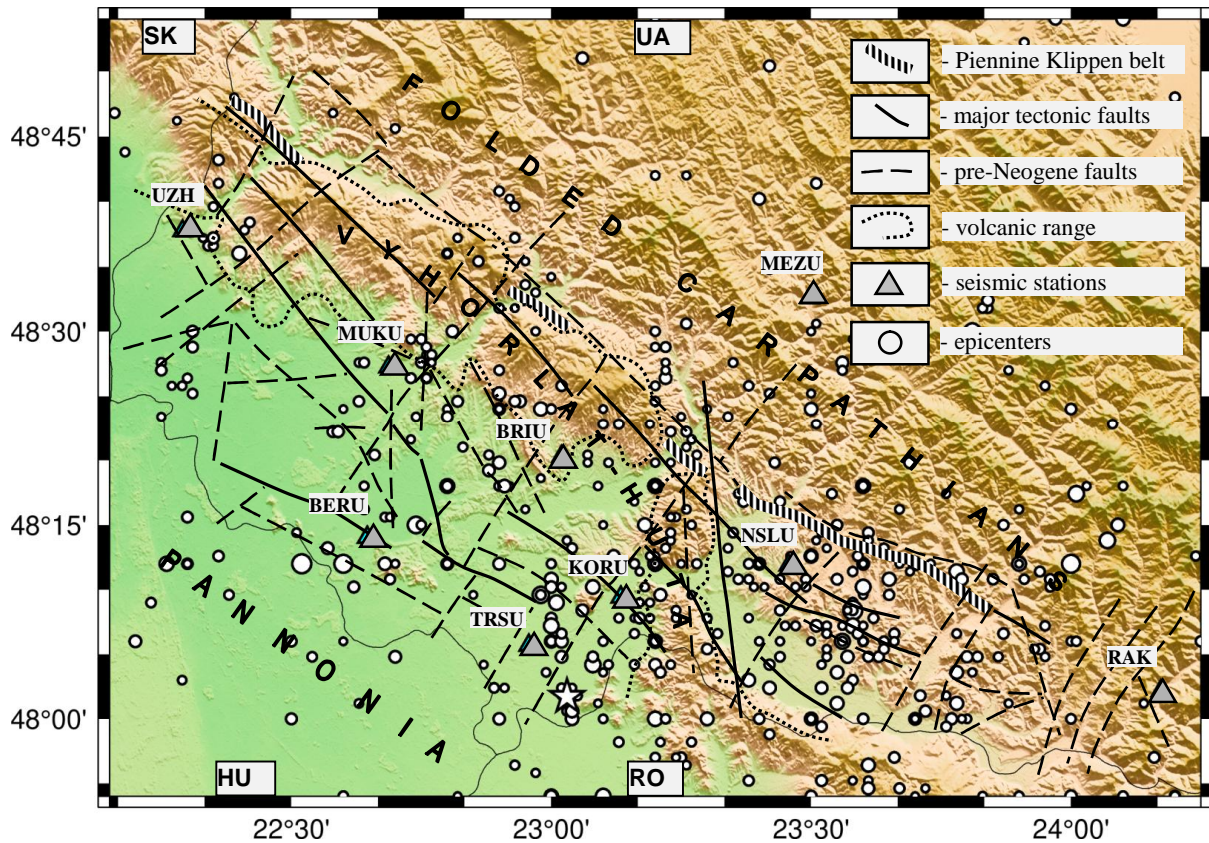


Fig. 1. The Transcarpathian region of Ukraine, its seismicity ($0.7 \leq M_L \leq 5.6$) during 1961–2015, location of the 2013–2015 Trosnyk series (hollow star) and elements of the local tectonics according to [Khomenko, 1971, 1987]

It is clear that probabilistic characteristics (in particular, the cross-correlation function) are especially useful for comparing records of weak earthquakes, whose phases are fuzzy or even unrecognizable, with records of stronger ones, with clearer phases. However, as for the series near the village of Trosnyk in 2013–2015, even a cursory analysis showed that some of the earthquakes were so weak and with such a low signal-to-noise ratio in the records that the correlation maxima sometimes did not even reach the significance threshold of 0.7–0.8, which is minimally acceptable (in the absence of significant secondary maxima) in this kind of work. Such earthquakes are usually neglected.

Taking this into account and in order not to waste the valuable material of seismological observations in the region with a relatively low level of seismic activity, we propose new approaches to improve the reliability of phase arrivals. They are based on adaptive filtering of raw records in order to reduce the influence of correlated

noise. They also include the application of the maximum correlation criterion in combination with the minimum of shift, as well as the use of the intervals between P -wave arrivals of the same earthquakes at different stations.

Identification and verification of differential arrivals

The accuracy of the final coordinates of the foci under all other similar conditions (velocity model, etc.) depends not so much on the method used, as on the accuracy of the phase arrivals. At first glance, the task of identifying the differential arrivals may seem simple and even trivial (Fig. 2). However, the reasons discussed in the introduction prove that this is not applied to the series of earthquakes near the village of Trosnyk. The procedure for estimation of the differential arrivals consisted of several steps, or even their cycles, if some arrivals did not pass verification.

At the beginning, the identification of earthquakes belonging to the series was carried out by evaluating the similarity of the waveforms of all events that, according to the bulletin [Verbickij et al., 2014; Verbitsky et al., 2014, 2016], occurred in this epicenter zone during 2013–2015. For this purpose, records at the nearest stations with the highest signal-to-noise ratio (TRSU, KORU, BRIU, etc.) were used. In order to obtain the most constrained final locations (in particular to reduce the influence of network configuration), we tried to use arrivals at as many stations in Romania, Slovakia, and Hungary located closest to the epicenter area (but not listed in the bulletins) as possible. The records (although not of all stations) were available in direct access in the international databases of seismological information IRIS, ORFEUS and GeoForschungsZentrum.

On the other hand, the number of stations was limited by the condition that each of them had records

of all 17 earthquakes in the series. Indeed, for different sets of stations, the inaccuracy of the velocity model affects the final coordinates differently. This is true for both absolute and relative ones. Although, of course, the latter were of primary interest for us. Such a complete (or almost complete) set of records, primarily for technical reasons, was available only at stations TRSU, KORU, NSLU (Ukraine), KOLS (Slovakia), BMR, CJR (Romania), LTVH and PSZ (Hungary). It is also clear that it made no sense to include in the analysis the records of such relatively weak earthquakes at stations at epicenter distances greater than a few hundred kilometers. However, the PSZ station (at a distance of more than 230 km) turned out to be a certain exception here, apparently due to both the favorable conditions of registration and the quality of the equipment (the station is operated by the GeoForschungsZentrum).

Table 1

Bulletin hypocenter parameters of the 2013–2015 Trosnyk earthquakes [Verbickij et al., 2014; Verbitsky, et al., 2014, 2016]

| Event number | Day | Time, hh:mm:ss | Lat., (°N) | Lon., (°E) | Depth, km | M_{SH} | M_L | K_p |
|--------------|--------------|----------------|------------|------------|-----------|----------|-------|-------|
| 1 | 13(Jul) 2013 | 12:18:18.0 | 48.03 | 23.04 | 13.8 | 1.3 | 1.6 | 6.8 |
| 2 | 5(Dec) | 22:17:29.1 | 48.02 | 23.05 | 4.6 | 0.8 | 1.0 | 6.0 |
| 3 | 15(Nov) 2014 | 02:42:24.8 | 48.03 | 23.04 | 13.9 | 2.4 | 2.5 | 8.8 |
| 4 | | 03:02:00.7 | 48.01 | 23.03 | 12.9 | 1.7 | 1.9 | 7.5 |
| 5 | | 03:15:07.4 | 48.00 | 23.04 | 9.8 | 2.4 | 2.5 | 9.0 |
| 6 | | 05:47:10.9 | 48.01 | 23.04 | 11.8 | | 1.4 | |
| 7 | | 19:41:57.5 | 48.00 | 23.03 | 12.0 | | 1.0 | |
| 8 | 22(Nov) | 00:26:33.6 | 48.01 | 23.05 | 13.0 | | 0.7 | |
| 9 | 26(Nov) | 10:49:52.4 | 48.01 | 23.04 | 13.0 | 2.3 | 2.4 | 9.0 |
| 10 | 9(Dec) | 23:56:30.0 | 48.04 | 23.04 | 14.0 | | 1.0 | |
| 11 | 16(Dec) | 16:00:01.6 | 48.03 | 23.02 | 15.1 | 1.3 | 1.7 | 7.1 |
| 12 | 13(Jan) 2015 | 09:05:12.3 | 48.03 | 23.05 | 8.9 | 1.6 | 1.8 | 7.6 |
| 13 | 06(Feb) | 02:11:39.4 | 48.04 | 23.02 | 15.1 | 1.6 | 1.8 | 7.4 |
| 14 | 15(Feb) | 14:35:13.5 | 48.04 | 23.04 | 15.2 | 1.6 | 2.0 | 7.3 |
| 15 | 15(Feb) | 17:47:05.0 | 48.04 | 23.03 | 15.0 | | 1.0 | |
| 16 | 05(Apr) | 11:16:12.1 | 48.05 | 23.02 | 16.9 | 1.4 | 1.6 | 6.5 |
| 17 | 13(Apr) | 22:04:54.8 | 48.02 | 23.04 | 12.7 | 1.2 | 1.4 | 6.7 |

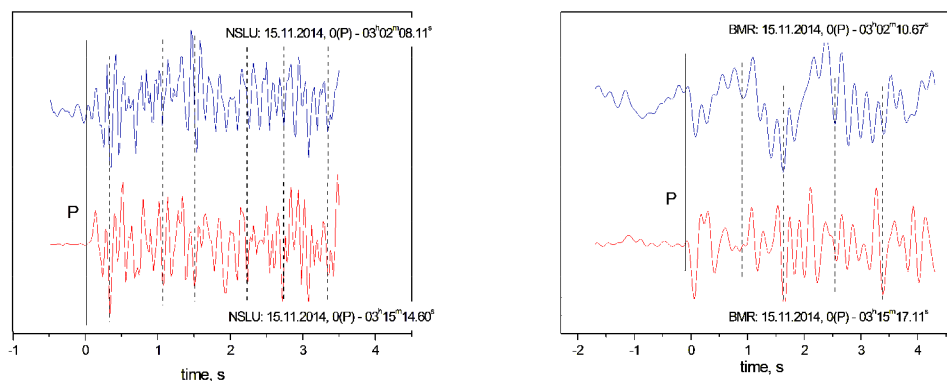


Fig. 2. Estimation of the differential arrivals of *P*-waves of Trosnyk earthquakes by taking into account the shift of the maximum of the cross-correlation function between the unfiltered records at the NSLU station and filtered in the passband from 0.5 to 5.5 Hz at the BMR station

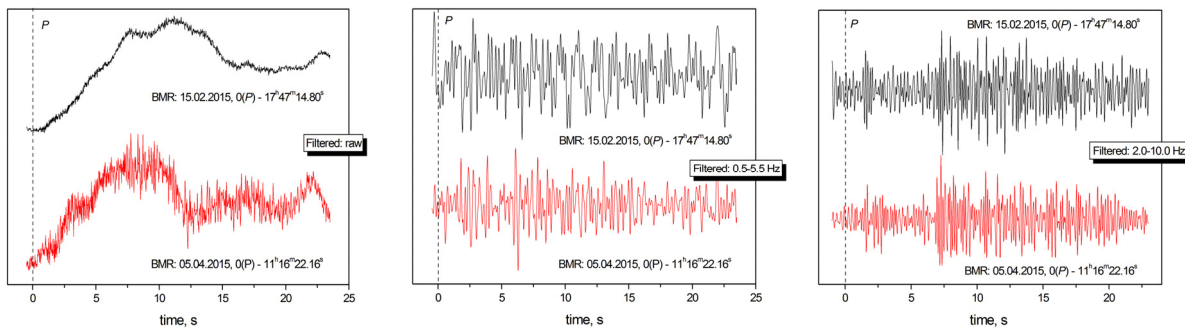


Fig. 3. Correlated noise in records of Trosnyk earthquakes at the BMR station in different frequency ranges

Next, at each of the stations, the portions of records that may contain the first arrivals were identified. When processing a large number of records, and especially with a low signal-to-noise ratio, and from a large number of stations, visual identification of the first arrivals is not only time-consuming and impractical, but often simply impossible. Therefore, the travel time to each of the stations (primarily those not listed in the bulletin) was first calculated for the main (strongest) earthquake of the series (15.11.2014, 3^h15^m7.4^s, $M_L = 2.5$, $M_{SH} = 2.4$, $Kp = 9.0$ [Verbitsky et al., 2014]) using the MEZU velocity model [Starodub & Gnyp, 1999]. The same model was later also used during estimation of the differential locations. The approximate arrival time for other earthquakes was calculated, by adding the travel time for the main earthquake to their bulletin source time [Verbickij et al., 2014; Verbitsky et al., 2014, 2016]. By adding a reasonable margin, variations in the real arrival time due to different location of sources (as well as due to inaccuracy of the model, source times, etc.) were taken into account.

In order to improve the signal-to-noise ratio, the 0.02 s records (at Ukrainian stations) and 0.01 s records (at other stations) were band-pass filtered from 0.5 to 5.5 Hz at this stage.

The length of the records was chosen in such a way that it contained the *S*-wave. In all components, it is usually of a much larger amplitude (and, accordingly, the signal-to-noise ratio) than *P*-wave. It is quite understandable that in this case the maximum correlation corresponded to *S*-wave. Variations in the interval between the first *P*- and *S*-waves due to the different locations were taken into account already at the next step by limiting the length of the record so that it no longer contained the *S*-wave.

The inaccuracy of identification of the first arrivals of the *S*-wave even for the strongest earthquakes of the series could only be much larger than the variations of their delay relative to *P*- wave. So, the differential coordinates of the earthquakes were estimated using only the first arrivals of the *P*-wave. Taking into account the *S*-wave in this

situation would lead only to significant distortion of coordinates.

In the works [Gnyp, 2010; Gnyp & Malyskiy, 2021], the differential arrivals of the *P*-wave were estimated relative to the so-called *master event*, which is the most common practice in similar studies [Shearer, 1997; Shearer et al., 2005]. However, the arrivals were determined not directly (taking into account the shift of the maximum correlation with the master event), but through the chain of pairs with the largest value of the maximum, according to the principle of the so-called single-linkage clustering [Sibson, 1973].

Since the signal-to-noise ratio in most records of the Trosnyk series was very low, the correlation was significantly affected by the so-called correlated noise (Fig. 3). Indeed, filtering in the pass-band between 0.5 and 5.5 Hz eliminated some of them, but not all, as can be seen from Fig. 4. So, in order to further reduce the effect of noise, it was decided to choose another, more optimal frequency range.

The problem here was that noise can be present in the same frequency range as the signal itself. So choosing a filter band was a trade-off between removing noise and preserving as much information about the signal as possible. The presence of correlated noise (as well as the displacements corresponding to it) was detected by calculating the correlation between the portions of the records that did not contain a signal (before the arrival of the *P*-wave) (Fig. 4). Differential arrivals in pairs with correlated noise were not determined. In this case, other pairs were taken, albeit with a lower correlation.

Since it is impossible to completely eliminate the effect of correlated noise, while maintaining the principle of single-linkage clustering, the criterion of the correlation maximum was modified to include the minimum departure from the calculated arrival time. Furthermore, preference was given to pairs with arrivals corresponding to azimuth variations of *P*-wave delays of the same events at one station relative to the other, chosen as a reference (Fig. 5) [Gnyp & Malyskiy, 2021].

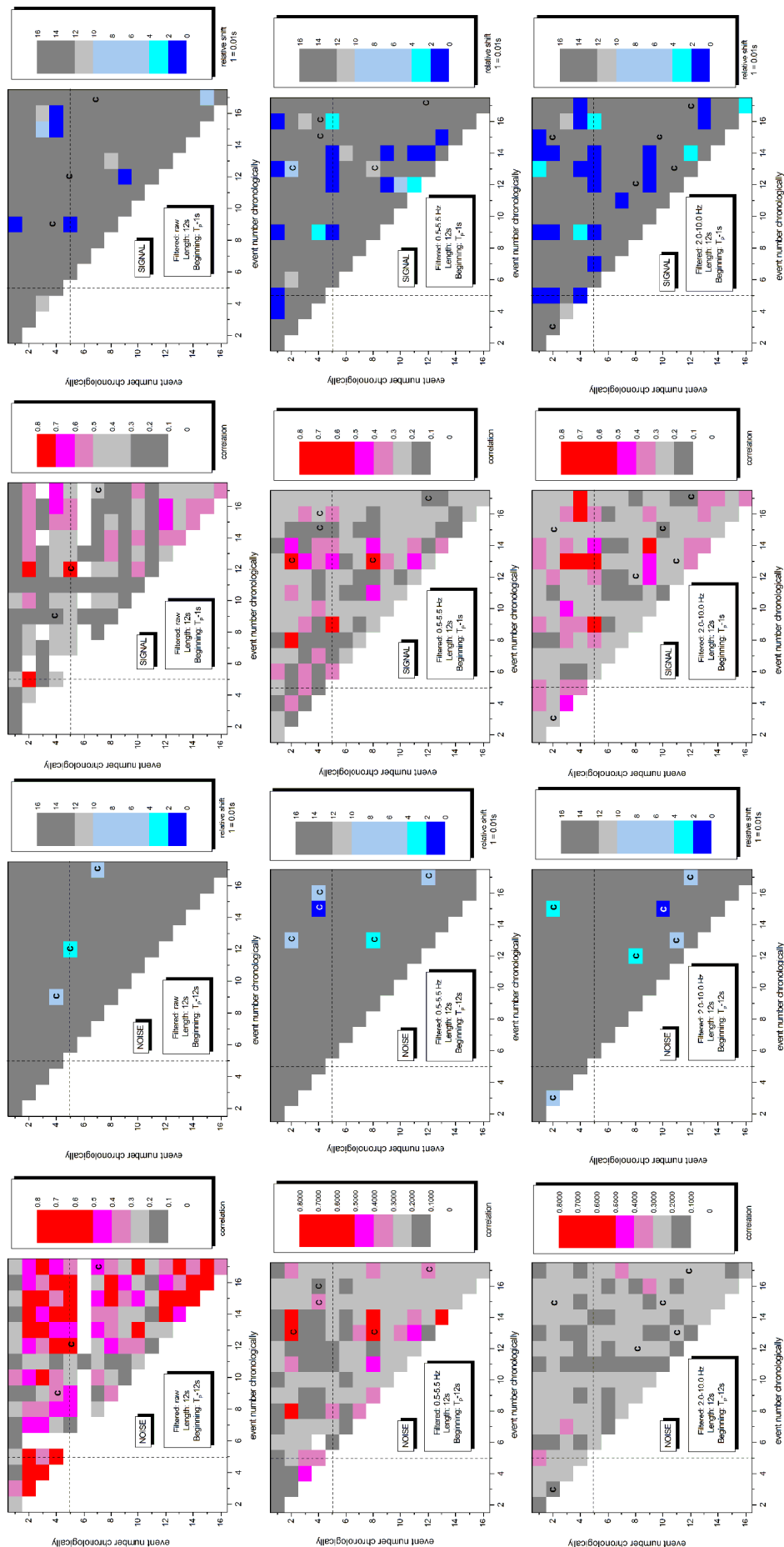


Fig. 4. Effect of correlated noise in different frequency bands – color map presentation of the maximum correlation between records at the CJR station.

At the top row – the maxima of the cross-correlation function between the portions of unfiltered (raw) records 12 s long and beginning at 12 s before the arrival of the *P*-wave (*T_p*-12, NOISE), their corresponding shifts, the maxima between portions beginning at 1 s before the differential arrival of the *P*-wave (*T_p*-1, SIGNAL), and the corresponding shifts. In the middle row – the maxima and shifts between records filtered in the passband between 0.5 and 5.5 Hz, and at the bottom row – between 0 and 10.0 Hz, on the right are their corresponding shifts. Pairs with minimal (less than 0.1 s) shift of maximum correlation between portions containing noise are indicated with the letter *c*. Pairs with the main event (*master event*) are indicated with a dashed line

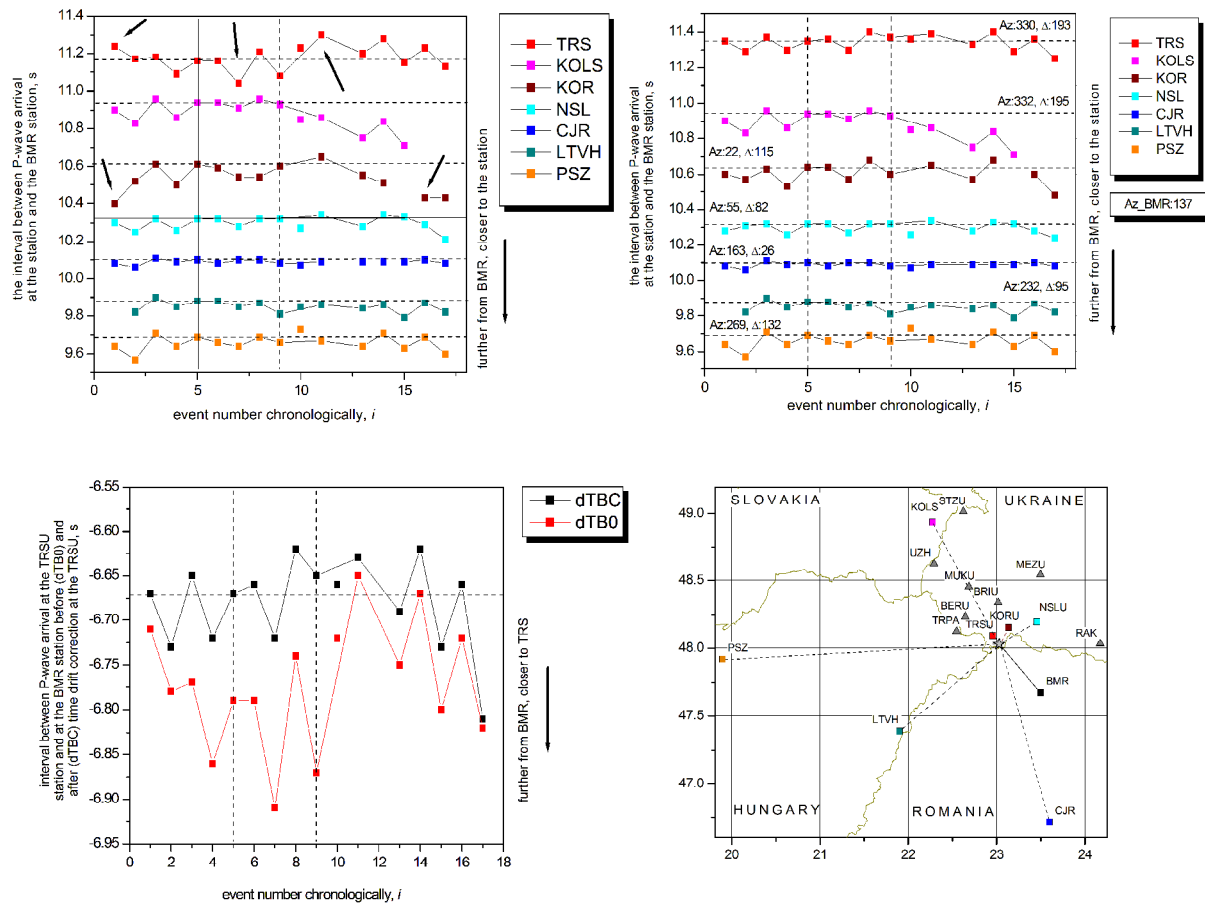


Fig. 5. Variations in the intervals between *P*-wave arrivals at the stations and the BMR station before (top left) and after (top right) correction of the time drift at the TRSU, NSLU, and KORU stations (relative to the conditional level)

The azimuths from the epicenter to the station are indicated on the upper right. Variations at the TRSU station (bottom left). The location of the stations (colored squares) relative to the epicenter (star) – bottom right. Gray triangles indicate the stations only used to determine the source mechanism

For each of the earthquakes, the delays were practically proportional to the difference in the distances between the source and the stations. Variations of the delays between earthquakes corresponded to a change in the location of one earthquake relative to another (increase – to a greater relative distance from the station, and vice versa). It was quite understandable that the variations should be of some orderly pattern, depending on the station azimuths and epicenter distances. The departure from the pattern might indicate a problem with estimated arrivals. From irregularities in the variations of delays in the work [Gnyp & Malytskyy, 2021], in particular, a significant time drift was found at some stations of the Ukrainian network (at the BRIU station, for example, it even amounted to 0.7 s).

To account for the time drift, a special algorithm was developed in the current work in which the corrected time is calculated assuming a linear rate of

the drift between synchronizations by radio signals (Fig. 5).

Estimation of differential locations

The differential coordinates of the 2013-2015 Trosnyk series were calculated using the well-known FASTHYPO algorithm [Herrmann, 1979] and the horizontally-layered velocity model MEZ [Starodub & Gnyp, 1999] (Fig. 6). Although proposed a few decades ago, the algorithm still remains very effective and reliable. Simultaneously, the source-specific station terms were calculated by iteratively relocating the earthquakes with accounting each time for the averaged residuals between the “observed” (in the first iteration – differential) and calculated travel times ($t_o - t_c$). To minimize the effect of eventual errors in the differential arrivals, especially of the weaker earthquakes, the terms were estimated only

for the strongest ones (2–6, 9, 11–14, Fig. 6, Table 1). The dispersion of residuals at the same stations turned out to be insignificant, and the process itself converged only after two iterations, which (first and second) can indicate both the reliability of the initial (differential) arrivals (at least for the strongest earthquakes) and to the stability of the obtained solution (final coordinates and source times, Table 2).

As expected, the terms were the largest for the most distant stations (Fig. 6). In particular, for the PSZ station (at an epicenter distance of more than 230 km), the correction was almost -1.5 s. Indeed, in different directions from the epicenter (Figs. 5, 6), the variations in the velocities of seismic waves only increase with distance, which cannot be taken into account in one model.

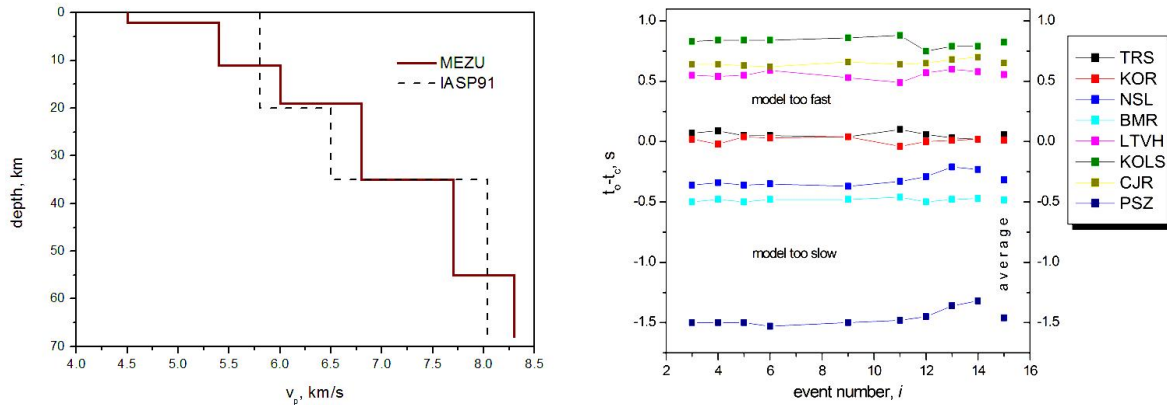


Fig. 6. Model MEZ [Starodub et al., 1999] used for relocation (in comparison with the model IASP91). Source specific station terms obtained after 2 iterations

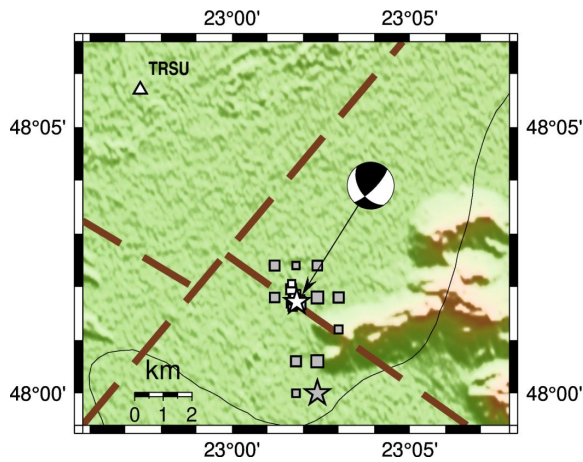


Fig. 7. The Bulletin [Verbickij et al., 2014; Verbitsky et al., 2014, 2016] epicenters of the series the (gray squares, Table 1) and calculated using the differential arrivals and taking into account the source-specific station terms (white, Table 2), and the mechanism of the strongest earthquake according to the polarities of the first arrivals of the *P*-wave at 16 stations

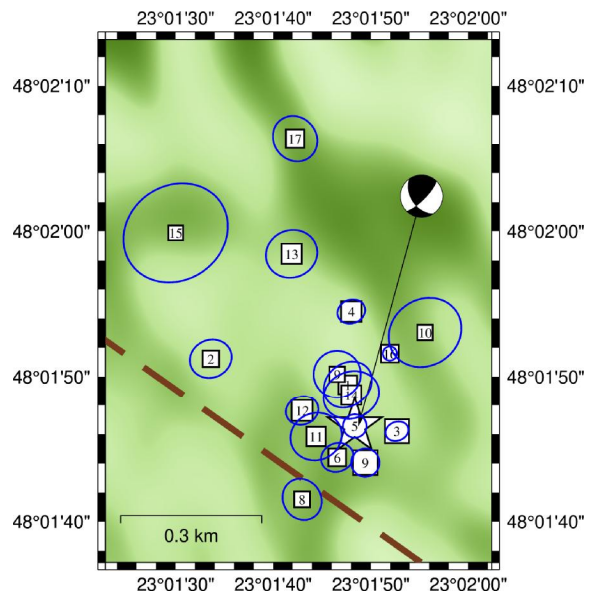


Fig. 8. Epicenters of the Trosnyk series calculated using differential arrivals at the full set of stations (Table 2) with error ellipses (blue), and the focal mechanism of the strongest earthquake

Stars show the strongest earthquake. Thick dashed lines are the faults of the pre-Neogene basement [Khomenko, 1971, 1987]. On the lower right, there is the western slope of the Yulivska (Klynovetska) mountain, which belongs to the Vyhorlat-Guta volcanic range

The thick dashed line is a fault of the pre-Neogene basement [Khomenko, 1971, 1987]

As also expected, the differential locations of the series were scattered within a much smaller area than in the bulletin [Verbickij et al., 2014; Verbitsky et al.,

2014, 2016] (Figs. 7, 8). The greatest distance between the epicenters was less than 1 km. The depths of the foci turned out to be almost the same, in the range between 10.45 and 10.92 km. These depths, however, could be controlled by the presence of a boundary between layers with contrasting velocities at a depth of 11 km in the MEZ model (Fig. 6). In the horizontal plane, the area of the differential epicenters is clearly elongated in the direction from the northwest to the southeast (Fig. 8). It is completely consistent with the character of the variations in the *P*-wave arrival delays at the stations relative to the BMR station (Fig. 5). Indeed, their largest amplitude is observed at stations along the BMR-TRSU axis (exactly from NW to SE), while the smallest in the perpendicular direction of NSLU-LTVH. If the axis of horizontal elongation were directed along the NSLU-LTVH axis, then it would be the opposite – the largest variations would be at stations exactly along this direction.

Root-mean-square errors of absolute locations, after taking into account station terms, retained little physical meaning (except possibly for relative locations). Therefore, the so-called *jack-knife* test was performed in order to assess the influence of the distribution of stations around the epicenters (as well as possible gross errors in arrivals). During the test, the coordinates of foci are calculated by dropping one station at a time from the full set of stations [Efron, 1982; Waldhauser & Ellsworth, 2000]. The largest variations of coordinates relative to the full set of stations were observed for the weakest earthquakes (8, 10, 11, 15, 17) (Table 2), which is quite natural

and may indicate the presence of errors in the differential arrivals at some stations (Fig. 9).

It was impossible to further refine their arrivals, due to the low level of correlation between the records of these earthquakes with others. So, another version of the final locations was proposed. They were obtained as a result of the jack-knife test without the KOLS station, which caused the largest root mean square error for most earthquakes (Fig. 10, 11, Table 3). The omitting of the KOLS station appeared to be justified by somewhat anomalous behavior of the delays of the first *P*-waves at it relative to the BMR station (Fig. 5) (especially after the beginning of 2015), which may indicate a problem with the time at it. In addition, there were no records of the last two earthquakes of the series at the station, which contradicted the already mentioned condition of the same network configuration for all earthquakes. On the other hand, as can be seen from the diagram in Fig. 5, the azimuth of the KOLS station almost coincides with the TRSU station. Thus, the much clearer first arrivals at the latter “controlled” the epicenter distance in this direction much more reliably. Fig. 8 and 10 show that in the end only the location of the 15th earthquake changed quite significantly. It “moved” much closer to the main group, in which the relative locations of the epicenters remained practically the same. It is also worth noting that the 15th earthquake occurred exactly when the problem with time probably emerged at the KOLS station (Fig. 5), which later even probably led to its suspension.

Table 2

Relocated hypocenter parameters of the 2013–2015 Trosnyk earthquakes. Magnitude M_L is indicated according to [Verbickij et al., 2014, Verbitsky, et al., 2014, 2016]

| No | Day | Time, hh:mm:ss | Lon., (°E) | Lat., (°N) | Depth, km | S_{time} , km | $S_{lon.}$, km | $S_{lat.}$, km | $S_{depth.}$, km | <i>RMS</i> | M_L |
|----|--------------|----------------|------------|------------|-----------|-----------------|-----------------|-----------------|-------------------|------------|-------|
| 1 | 13(Jul) 2013 | 12:18:18.38 | 23.0299 | 48.0304 | 10.64 | 0.01 | 0.1 | 0.1 | 0.11 | 0.025 | 1.6 |
| 2 | 5(Dec) | 22:17:28.62 | 23.0260 | 48.0309 | 10.60 | 0.01 | 0.08 | 0.09 | 0.10 | 0.023 | 1.0 |
| 3 | 15(Nov) 2014 | 02:42:25.17 | 23.0313 | 48.0295 | 10.49 | 0.01 | 0.04 | 0.04 | 0.05 | 0.013 | 2.5 |
| 4 | | 03:02:01.25 | 23.0300 | 48.0318 | 10.52 | 0.01 | 0.06 | 0.05 | 0.07 | 0.016 | 1.9 |
| 5 | | 03:15:07.73 | 23.0301 | 48.0296 | 10.53 | 0.01 | 0.05 | 0.05 | 0.06 | 0.015 | 2.5 |
| 6 | | 05:47:11.27 | 23.0296 | 48.0290 | 10.53 | 0.01 | 0.07 | 0.07 | 0.08 | 0.020 | 1.4 |
| 7 | | 19:41:58.03 | 23.0296 | 48.0306 | 10.45 | 0.01 | 0.10 | 0.11 | 0.12 | 0.028 | 1.0 |
| 8 | 22(Nov) | 00:26:34.09 | 23.0286 | 48.0282 | 10.46 | 0.01 | 0.09 | 0.09 | 0.10 | 0.020 | 0.7 |
| 9 | 26(Nov) | 10:49:52.97 | 23.0304 | 48.0289 | 10.67 | 0.01 | 0.06 | 0.06 | 0.07 | 0.018 | 2.4 |
| 10 | 9(Dec) | 23:56:30.29 | 23.0321 | 48.0314 | 10.69 | 0.02 | 0.14 | 0.15 | 0.18 | 0.038 | 1.0 |
| 11 | 16(Dec) | 16:00:02.26 | 23.0290 | 48.0294 | 10.60 | 0.01 | 0.11 | 0.10 | 0.13 | 0.031 | 1.7 |
| 12 | 13(Jan) 2015 | 09:05:12.13 | 23.0286 | 48.0299 | 10.74 | 0.01 | 0.06 | 0.06 | 0.07 | 0.018 | 1.8 |
| 13 | 06(Feb) | 02:11:39.85 | 23.0283 | 48.0329 | 10.80 | 0.01 | 0.11 | 0.10 | 0.12 | 0.030 | 1.8 |
| 14 | 15(Feb) | 14:35:13.91 | 23.0300 | 48.0302 | 10.92 | 0.01 | 0.11 | 0.10 | 0.13 | 0.032 | 2.0 |
| 15 | 15(Feb) | 17:47:05.39 | 23.0250 | 48.0333 | 10.81 | 0.03 | 0.21 | 0.23 | 0.27 | 0.057 | 1.0 |
| 16 | 05(Apr) | 11:16:12.74 | 23.0311 | 48.0310 | 10.64 | 0.00 | 0.03 | 0.03 | 0.04 | 0.009 | 1.6 |
| 17 | 13(Apr) | 22:04:55.16 | 23.0284 | 48.0351 | 10.68 | 0.01 | 0.09 | 0.09 | 0.11 | 0.025 | 1.4 |

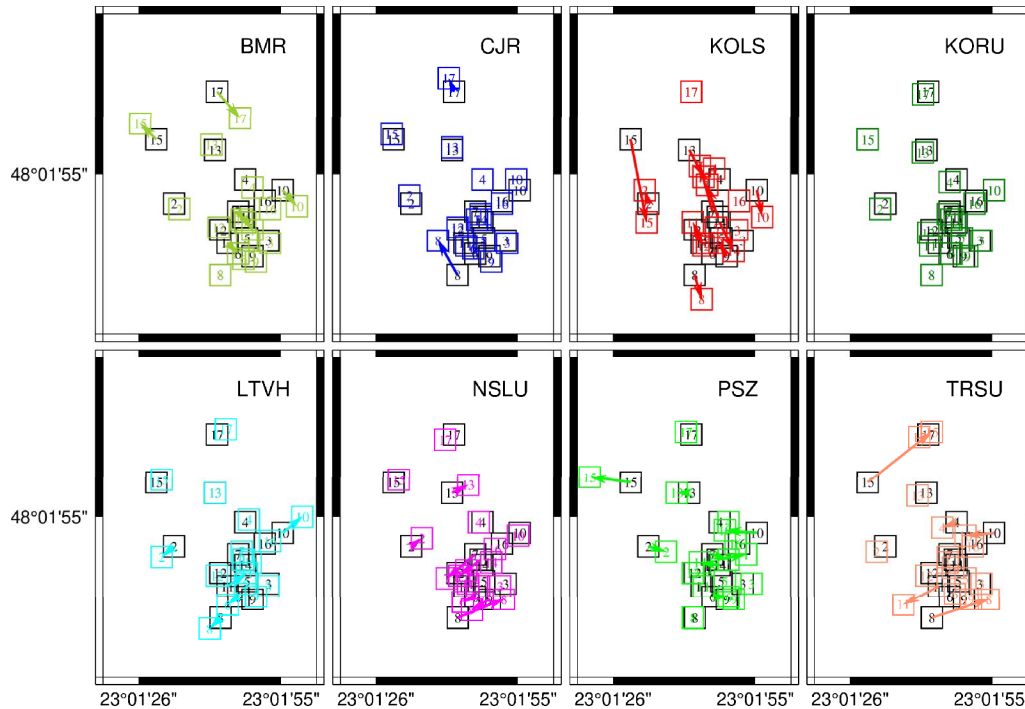


Fig. 9. Epicenters of Trosnyk earthquakes calculated using the full set of stations (black squares) and without one station (color squares) (the so-called *jack-knife* test)

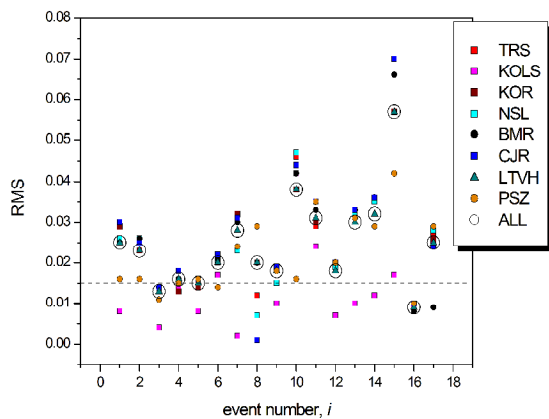


Fig. 10. Root mean square errors for the full set of stations (ALL) and for the set reduced by one station each time (the *jack-knife* test)

Focal mechanism of the strongest earthquake

It could be confidently concluded that the focal mechanism of all earthquakes was the same, considering the high degree of correlation between the waveforms of the series at the same stations, as well as the same sign of the *P*-wave arrivals (at least at those stations where it could be clearly identified).

Since even the strongest earthquake of 15.11.2014 was still too weak ($M_L = 2.5$), it was almost impossible to obtain metric estimates of its first pulses (duration and amplitude) at most stations. Indeed, the evaluation of metric parameters involves removing the frequency response of the instrument,

that is, filtering the raw record. If the amplitude of the first pulse is small, then this leads to such distortion that it is often impossible to identify it.

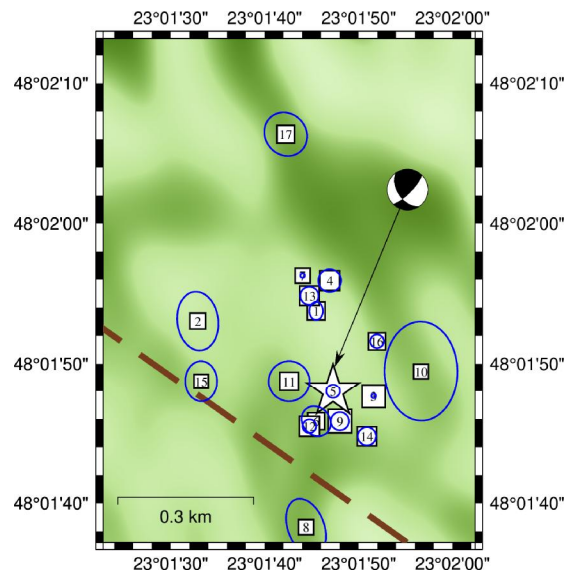


Fig. 11. Version of the final locations calculated without the KOLS station, which caused the largest errors (Fig. 10) for most earthquakes (Table 3), with error ellipses (blue), and the focal mechanism of the strongest earthquake

The thick dashed line is a fault of the pre-Neogene basement [Khomenko, 1971, 1987]

Therefore, the focal mechanism was estimated in the traditional way from the polarities of *P*-wave arrivals at 16 stations of the seismological networks of Ukraine, Romania, Hungary, and Slovakia (Fig. 12). The same MEZ velocity model was used to calculate the angles of emergence

(Figs. 5, 6). Records of strong teleseismic earthquakes with a known mechanism (and, therefore, the polarity of the first arrivals at the station) were used to detect eventual reversals in the polarity of the vertical component sensors at the stations.

Table 3

Version of hypocenter parameters of the 2013–2015 Trosnyk earthquakes relocated with omitting of the KOLS station (magnitude M_L is indicated according to [Verbickij et al., 2014; Verbitsky et al., 2014, 2016])

| No | Day | Time, hh:mm:ss | Lon., (°E) | Lat., (°N) | Depth, km | S_{time} , km | S_{lon} , km | S_{lat} , km | S_{depth} , km | RMS | M_L |
|----|--------------|----------------|------------|------------|-----------|-----------------|----------------|----------------|------------------|-------|-------|
| 1 | 13(Jul) 2013 | 12:18:18.38 | 23.0293 | 48.0316 | 10.77 | 0.00 | 0.03 | 0.04 | 0.04 | 0.008 | 1.6 |
| 2 | 5(Dec) | 22:17:28.62 | 23.0258 | 48.0314 | 10.66 | 0.01 | 0.09 | 0.13 | 0.13 | 0.025 | 1.0 |
| 3 | 15(Nov) 2014 | 02:42:25.17 | 23.0310 | 48.0299 | 10.54 | 0.00 | 0.01 | 0.01 | 0.02 | 0.004 | 2.5 |
| 4 | | 03:02:01.25 | 23.0297 | 48.0322 | 10.56 | 0.01 | 0.05 | 0.05 | 0.06 | 0.014 | 1.9 |
| 5 | | 03:15:07.73 | 23.0298 | 48.0300 | 10.58 | 0.00 | 0.03 | 0.03 | 0.04 | 0.008 | 2.5 |
| 6 | | 05:47:11.27 | 23.0293 | 48.0294 | 10.58 | 0.01 | 0.06 | 0.06 | 0.08 | 0.017 | 1.4 |
| 7 | | 19:41:58.03 | 23.0289 | 48.0323 | 10.63 | 0.00 | 0.01 | 0.01 | 0.01 | 0.002 | 1.0 |
| 8 | 22(Nov) | 00:26:34.09 | 23.0290 | 48.0273 | 10.38 | 0.01 | 0.09 | 0.13 | 0.12 | 0.020 | 0.7 |
| 9 | 26(Nov) | 10:49:52.97 | 23.0300 | 48.0294 | 10.73 | 0.00 | 0.04 | 0.04 | 0.05 | 0.010 | 2.4 |
| 10 | 9(Dec) | 23:56:30.29 | 23.0324 | 48.0304 | 10.60 | 0.02 | 0.16 | 0.22 | 0.23 | 0.042 | 1.0 |
| 11 | 16(Dec) | 16:00:02.26 | 23.0285 | 48.0302 | 10.69 | 0.01 | 0.09 | 0.09 | 0.11 | 0.024 | 1.7 |
| 12 | 13(Jan) 2015 | 09:05:12.13 | 23.0291 | 48.0293 | 10.67 | 0.00 | 0.03 | 0.03 | 0.03 | 0.007 | 1.8 |
| 13 | 06(Feb) | 02:11:39.85 | 23.0291 | 48.0319 | 10.69 | 0.00 | 0.04 | 0.04 | 0.04 | 0.010 | 1.8 |
| 14 | 15(Feb) | 14:35:13.91 | 23.0308 | 48.0291 | 10.80 | 0.01 | 0.04 | 0.04 | 0.05 | 0.012 | 2.0 |
| 15 | 15(Feb) | 17:47:05.39 | 23.0259 | 48.0302 | 10.53 | 0.01 | 0.07 | 0.09 | 0.10 | 0.017 | 1.0 |
| 16 | 05(Apr) | 11:16:12.74 | 23.0311 | 48.0310 | 10.64 | 0.00 | 0.03 | 0.03 | 0.04 | 0.009 | 1.6 |
| 17 | 13(Apr) | 22:04:55.16 | 23.0284 | 48.0351 | 10.68 | 0.01 | 0.09 | 0.09 | 0.11 | 0.025 | 1.4 |

Discussion

The most obvious result, which follows from the high degree of correlation between the waveforms of earthquakes near the village of Trosnyk in 2013–2015, is that they belonged to the class of so-called recurrent (or similar) earthquakes and most likely had a common rupture plane, which in one way or another should be related to local fault tectonics.

Such a long duration of the series is probably typical for the western part of the Transcarpathians, where a series of similar earthquakes of comparable duration was identified near the village of Michalovce in Slovakia (on the border with Ukraine) in 2003 and 2009, near Mukacheve in 2005–2006 [Gnyp, 2010], etc. In the other part of the region (approximately to the east of the north-south branch of the Vyhorlat-Huta ridge), the duration of the series usually does not exceed several weeks, such as the series of several hundred (!) quite strong for the Transcarpathians ($M_L \leq 3.5$) recurrent earthquakes near Teresva in July–August 2015 [Gnyp & Malyskyy, 2021]. R. S. Pronyshyn was one of the first to point

out the differences in the regime and character of seismicity in different parts of Transcarpathians several decades ago [Pronishyn & Pustovitenko, 1982]. The different duration of tectonic stress relaxation on the same fault plane can be a consequence of various factors. They include different geological structure and, accordingly, different rheological properties of the seismogenic medium, tectonic origin of earthquakes (relation to other types and classes of tectonic structures), as well as different tectonic regime (distribution of stress and strain fields, rate of stress accumulation and relaxation), or other reasons (such as temperature) that still require further clarification.

If sources of recurrent earthquakes by definition should belong to the same rupture plane, then a characteristic feature of the 3D presentation of differential hypocenters in Trosnyk (Fig. 13) can be considered their clear gravitating to an almost horizontal plane. It is, however, difficult to relate to one of the nodal planes of the focal mechanism estimated in the work (Fig. 12) due to the large angles of dip in both ($\sim 50^\circ$ and $\sim 80^\circ$). However, as already mentioned, small depth variations could be caused by

the boundary between layers with different velocities at a depth of 11 km in the MEZ model, or by large depth errors (Tables 2, 3), especially for weaker earthquakes. If, as during determining station terms, only stronger earthquakes (2–6, 9, 11–14, Table 1–3) were taken into account, then the plane (Fig. 13) to which the hypocenters gravitate dips almost exactly in the same direction as the nodal plane of the focal mechanism (Fig. 12) with a strike of $\sim 150^\circ$, a dip of $\sim 50^\circ$ and a rake of $\sim 20^\circ$, and is inclined oppositely to the second of the planes. Based on this, it could be assumed that the first of the planes corresponds to the actual rupture, and the mechanism can be classified as a mixed type – a left-lateral slip with a significant component of thrust. Most of the mechanisms in this part of the region, presented in particular in [Malyskyy et al., 2017, 2017], also belong to this type. Beyond that, the area of differential epicenters was elongated in almost the same direction (Fig. 8), and the largest variations in *P*-wave delays were observed at the stations in this direction relative to the BMR station (Fig. 5).

The plane with a strike of $\sim 150^\circ$ can also be associated with the nearest pre-Neogene basement fault [Khomenko, 1971, 1987] with a close orientation of $\sim 120^\circ$. In addition, the epicenter of the strongest earthquake was located almost exactly on this fault (Fig. 7–9).

However, there is another almost perpendicular fault (Fig. 7) very close by, some two kilometers to

the east. Its direction is $\sim 30^\circ$ to the northeast, which is close to azimuth of $\sim 60^\circ$ of another nodal plane of the mechanism [Khomenko, 1971, 1987]. Considering the probability of a large error in the absolute coordinates of the series, it is also impossible to rule out its connection with this fault.

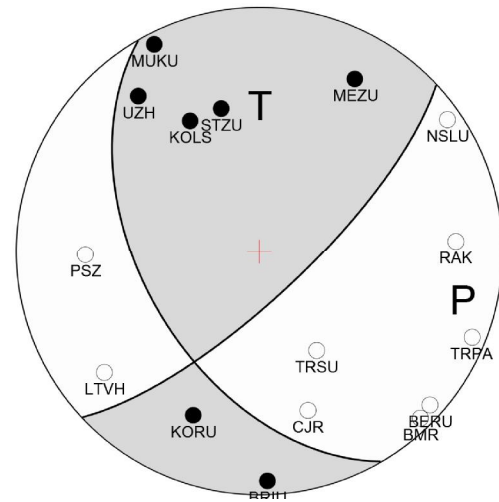


Fig. 12. Focal mechanism of the strongest earthquake estimated from polarities of first *P*-waves at 16 stations and using the MEZ velocity model for calculation of the angles of emergence: strike – $\sim 150^\circ$, dip – $\sim 50^\circ$, rake – $\sim 20^\circ$

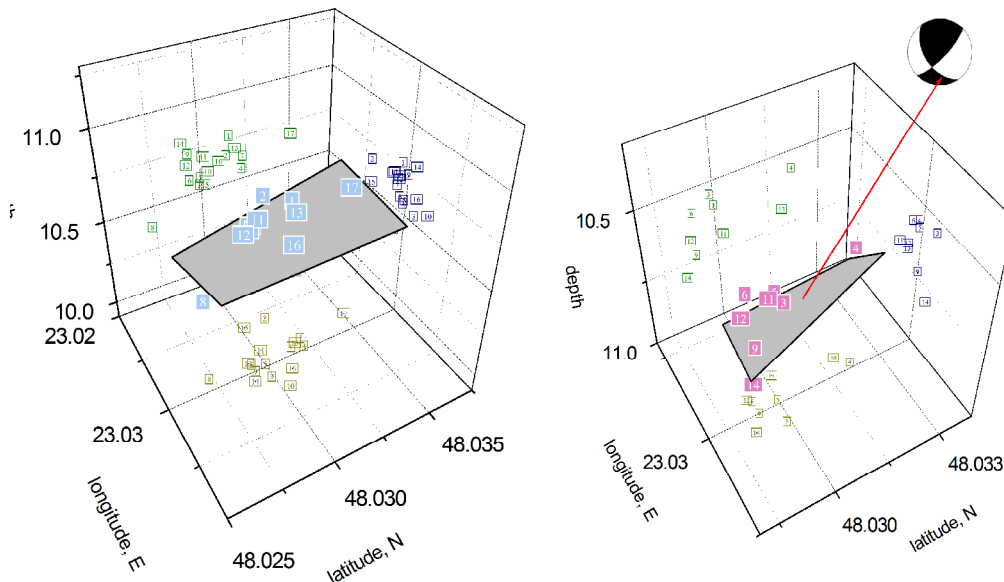


Fig. 13. 3D interpretation of the differential hypocenters near Trosnyk: on the left – all 17 hypocenters of the series are approximated by a plane constructed by the method of correlation grids [Davis, 1986]; on the right – only the hypocenters of the 9 strongest earthquakes. The red arrow indicates the most probable rupture plane in the focal mechanism

Fig. 1 and 7 show that the differential epicenters of the series were located almost on the western slope

of the Klynovetska (Yulivska) mountain, which belongs to the north-south branch of the Vyhorlat-

Huta volcanic ridge. This allows us to assume that the series might also be associated with intrusion fractures characteristic of the areas of volcanic activity.

The axis of compression in the focal mechanism of the Trosnyk earthquakes (Fig. 12) is oriented approximately in the east-west direction, which does not exactly correspond to the data on the orientation of compression in the western part of Transcarpathians in the direction to the northeast [Malyskyi et al., 2017]. However, in such cases, it should always be kept in mind that the general regional stress field interacts with the local fault system already present here. The directions of the stress axes in the mechanisms of individual earthquakes may diverge due to this. In this case this occurs from the northeast to the east, which is quite adequate, if we take into account the directions of local faults of the pre-Neogene basement (Figs. 1, 7, 8) [Khomenko, 1971, 1987].

Conclusions

Weak earthquakes are a very valuable material in seismological research, especially in regions with a low level of seismic activity, such as Transcarpathians, where strong earthquakes are rare. Improving the accuracy of the coordinates of such earthquakes is almost the most important condition for the possibility of their further tectonic interpretation. A way to solve this problem is to determine the differential arrivals of similar earthquakes, such as those that belonged to the 2013–2015 series near Trosnyk.

In the current work, the main efforts were focused on finding ways to improve the reliability of differential arrivals under the condition of very low signal-to-noise ratio in records of very weak similar earthquakes. To reduce the effect of correlated noise, adaptive filtering of records was proposed by calculating the correlation between segments of records containing only noise or both signal and noise. The maximum correlation criterion for estimation of the differential arrivals was modified to include a minimum shift relative to the calculated arrivals. In order to further improve the reliability of arrivals, the intervals between the first *P*-waves from the same earthquakes at pairs of stations were analyzed. As a result, more problematic arrivals were identified. A special algorithm was developed to account for time drift at some stations of the Carpathian network of the National Academy of Sciences of Ukraine. The differential coordinates of the foci of the 2013–2015 series in Trosnyk were calculated with the simultaneous calculation of source-specific station terms. Based on

3D interpretation of differential hypocenters, the actual rupture plane was identified in the common to the entire series focal mechanism. The tectonic interpretation of the differential locations and the focal mechanism allows us to assume that the series in Trosnyk is most likely related to the fault of the pre-Neogene basement parallel to the Carpathians, almost exactly where the epicenter of the strongest earthquake was. It is clear, however, that much more seismic material needs to be used to improve our understanding of the active tectonics of the region through the study of recurrent earthquakes, which can only be seen as a task for the future. The approaches proposed in the work can increase the amount of useful material and improve the reliability of the results.

Acknowledgments

The author expresses great gratitude to the head of the Department of Seismicity of the Carpathian Region of Ukraine of the Subbotin Institute of Geophysics of the National Academy of Sciences of Ukraine S. T. Verbytskyi and the leading engineer of the Department I. M. Nishchimenko for consultations and kindly providing the data of seismological observations.

Some figures were plotted using GMT [Wessel et al., 2013].

References

- Davis, J. C. (1986). *Statistics and Data Analysis in Geology*. John Wiley & Sons, Inc., Second edition.
- Efron, B. (1982). The Jackknife, the Bootstrap, and Other Resampling Plans. *SIAM*. <https://doi.org/10.1137/1.9781611970319>
- Gnyp, A. (2010). Refining locations of the 2005–2006 recurrent earthquakes in Mukacheve, West Ukraine, and implications for their source mechanism and the local tectonics. *Acta Geophysica* 58 (4), 587–603. <https://doi.org/10.2478/s11600-010-0006-9>
- Gnyp, A. (2013). Recovering Relative Locations of the 2005–2006 Mukacheve Earthquakes from Similarity of their Waveforms at a Single Station. *Acta Geophysica*, 61 (5), 1074–1087. <https://doi.org/10.2478/s11600-012-0096-7>
- Gnyp, A. (2014). On Reproducibility of Relative Locations of Recurrent Earthquakes Recovered from Similarity of their Waveforms at a Single Station. *Acta Geophysica*, 62 (6), 1246–1261. <https://doi.org/10.2478/s11600-013-0195-0>
- Gnyp, A., & Malyskyi, D., (2021). Differential and source terms locations of the 2015 Teresva (East Carpathians) series and their tectonic

- implications. *Acta Geophysica*, 69 (6), 2099–2112. <https://doi.org/10.1007/s11600-021-00655-w>, <https://rdocu.be/cyPNh>
- Harris, D. B. (1991). A waveform correlation method for identifying quarry explosions, *Bull. seism. Soc. Am.*, 81(6), 2395–2418. <https://doi.org/10.1785/BSSA0810062395>
- Harris, D. B., & Douglas, A. D. (2021). The geometry of signal space: a case study of direct mapping between seismic signals and event distribution. *Geophys. J. Int.*, 224, 2189–2208. <https://doi.org/10.1093/gji/ggaa572>
- Herrmann, R. B. (1979). FASTHYPO – a hypocenter location program. *Earthquake notes*, 50(2), 25–37. <https://doi.org/10.1785/gssrl.50.2.25>
- Khomenko, V. I. (1971). Deep Structure of the Transcarpathian Depression. *Naukova Dumka*. (in Ukrainian)
- Khomenko, V. I. (1987). Deep Structure of the South-West Edge of the East-European platform. *Naukova Dumka* (in Russian)
- Malytskyy, D. V., Obidina, O. O., Gnyp, A. R., Pavlova, A. Y., & Grytsai, O. D. (2017). Tectonic stresses in the area of Solotvyno deep, Eastern Carpathians, from focal mechanisms of local earthquakes. *16th International Conference on Geoinformatics – Theoretical and Applied Aspects, 15–17 May 2017, Kyiv, Ukraine, Conference Paper 11137_ENG*. <https://doi.org/10.3997/2214-4609.201701868>
- Malytskyy, D., Murovska, A., Obidina, O., Gnyp, A., Grytsai, O., Pavlova, A., & Pugach, A. (2017). Determining the stress field in earth's crust from source mechanisms of local earthquakes in the Transcarpatians. *Visnyk of Taras Shevchenko National University of Kyiv: Geology*, 3(78), 36–45. <http://doi.org/10.17721/1728-2713.78.05>
- Nadeau, R. M., & McEvilly, T. V. (1999). Fault slip rates at depth from recurrence intervals of repeating microearthquakes. *Science*, 285(5428), 718–721. <https://doi.org/10.1126/science.285.5428.718>
- Poupinet, G., Ellsworth, W. L., & Fréchet, J. (1984). Monitoring velocity variations in the crust using earthquake doublets: An application to the Calaveras Fault, California. *J. Geophys. Res.*, 89, B7, 5719–5731. <https://doi.org/10.1029/JB089iB07p05719>
- Pronishyn, R. S., & Pustovitenko, B. G. (1982). Some aspects of seismic “climate and weather” in the Transcarpathians. *Izv. Acad. Sci. USSR, Phys. Solid Earth*, 18, 74–81 (in Russian).
- Robinson, D. J., Sambridge, M., Sneider, R., & Hauser, J. (2013). Relocating a Cluster of Earthquakes Using a Single Seismic Station. *Bull. Seism. Soc. Am.*, 108(6), 3057–3072. <https://doi.org/10.1785/0120130004>
- Robinson, D. J., Sambridge, M., & Sneider, R. (2007). Constraints on coda wave interferometry estimates of source separation: The acoustic case. *Explor. Geophys.*, 38(3), 189–199. <https://doi.org/10.1071/EG07019>
- Robinson, D. J., Sneider, R., & Sambridge, M. (2007). Using coda wave interferometry for estimating the variation in source mechanism between double couple events. *J. Geophys. Res.*, 112(B12), B12302. <https://doi.org/10.1029/2007JB004925>
- Shearer, P. M. (1997). Improving local earthquake locations using L1 norm and waveform cross correlation: Application to the Whittier Narrows, California, aftershock sequence. *J. Geophys. Res.*, 102(B4), 8269–8283. <https://doi.org/10.1029/96JB03228>
- Shearer, P., Hauksson, E., & Lin, G. (2005). Southern California hypocenter relocation with waveform cross-correlation. Part 2: Results using source-specific station terms and cluster analysis. *Bull. Seism. Soc. Am.*, 95(3), 904–915. <https://doi.org/10.1785/0120040168>
- Sibson, R. (1973). SLINK: an optimally efficient algorithm for the single-link cluster method. *The Computer Journal. British Computer Society*, 16 (1): 30–34. <https://doi.org/10.1093/comjnl/16.1.30>
- Starodub, G., & Gnyp, A. (1999). Models of the Earth's Crust Structure in the East Carpathian Region determined from Inversion of Farfield *P*-waveforms. *Acta Geophysica Polonica*, 47(4), 375–400. Id. YADDA: bwmeta.element.baztech-article-BSL6-0006-0061
- Tibuleac, I. M., & Herrin, E. (1999). Lower mantle heterogeneity beneath the Caribbean Sea. *Science*, 285(5434), 1711–1715. <https://doi.org/10.1126/science.285.5434.1711>
- Verbytskyi, Yu. T., Gnyp, A. R., Narivna, M. M., Novotna, O. M., & Yarema, I. I. (2011). Identification of quarry blasts in the Carpathian region of Ukraine by the criterion of similarity of their waveforms. *Geodynamics*, 1(10), 103–109. <https://doi.org/10.23939/jgd2011.01.103>
- Verbickij, S. T., Pronishin, R. S., Verbickij, Yu. T., Chuba, M. V., Keleman, I. N., & Stetskiv, A. T. (2014). Seismological bulletin of Ukraine for 2013. *Sevastopol, NPC EHkosi-Gidrofizika*, 92–158 (in Russian).
- Verbitsky, S. T., Pronishin, R. S., Procopishin, V. I., Stetskiv, A. T., Chuba, M. V., Nischimenko, I. M., & Keleman, I. N. (2014). The seismicity of the Carpathians in 2014. *Scientific Notes of*

- V. I. Vernadsky Crimean Federal University. *Geography. Geology*, 27 (66), No. 2, 87–151 (in Russian).
- Verbitsky, S. T., Pronishin, R. S., Procopishin, V. I., Stetskiy, A. T., Chuba, M. V., Nischimenko, I. M., & Keleman, I. N. (2016), The seismicity of the Carpathians in 2015. *Scientific Notes of V. I. Vernadsky Crimean Federal University. Geography. Geology* 2(68), No. 4, 69–219 (in Russian).
- Waldhauser, F., & Ellsworth, L. W. (2000). A Double-Difference Earthquake Location Algorithm: Method and Application to the Northern Howard Fault. California. *Bull. Seism. Soc. Am.*, 90(6), 1353–1368. <https://doi.org/10.1785/0120000006>
- Wessel, P., Smith, W. H. F., Scharroo, R., Luis, J. F., & Wobbe, F. (2013). Generic mapping tools: improved version released. *EOS Trans. AGU*, 94, 409–410. <https://doi.org/10.1002/2013EO450001>

Андрій ГНИП

Карпатське відділення Інституту геофізики ім. С. І. Субботіна Національної академії наук України, вул. Наукова, 3Б, Львів, 79060, Україна, ел. пошта: agnyp.gm@gmail.com, <https://orcid.org/0000-0002-2612-4234>

ВИЗНАЧЕННЯ РІЗНИЦЕВИХ КООРДИНАТ І МЕХАНІЗМУ ВОГНИЩА ЗЕМЛЕТРУСІВ
ПОБЛИЗУ с. ТРОСНИК У ЗАКАРПАТТІ ПРОТЯГОМ 2013–2015 рр.:
МЕТОДИЧНІ АСПЕКТИ ТА АНАЛІЗ РЕЗУЛЬТАТІВ

Координати вогнищ серії слабких ($1,0 < M_L < 2,5$) схожих між собою (повторних) землетрусів, що відбувалися протягом 2013–2015 рр. поблизу с. Тросник на півдні Закарпаття, визначено за їхніми різницевиими (диференційними) вступами на українських, словацьких, угорських і румунських станціях з одночасним визначенням т. зв. епіцентрально-специфічних станційних поправок. З метою підвищення надійності різницевих вступів за умови дуже низького співвідношення сигнал/шум запропоновано адаптивне фільтрування записів для зменшення впливу корельованих шумів, модифікований критерій максимуму функції взаємної кореляції між відрізками записів із одночасним мінімумом зміщення відносно початкового обчисленого часу вступу, а також верифікацію вступів із використанням діаграм запізень вступів тих самих землетрусів на одних станціях відносно інших. Чутливість отриманого розв'язку до конфігурації мережі перевірено за допомогою т. зв. *jack-knife* тесту, коли координати вогнищ визначають, вилучаючи з повного набору станцій щоразу одну. За результатами 3D інтерпретації різницевих гіпоцентрів подальшу площину з азимутом простягання $\sim 150^\circ$ спільного для усіх землетрусів серії фокального механізму вогнища, визначеного за полярностями вступів *P*-хвиль на 16 станціях, ототожнено як площину розриву, а сам механізм класифіковано як лівосторонній зсув із компонентою насуву. Епіцентр найсильнішого землетрусу опинився майже точно на розломі донегенового фундаменту паралельного до дуги Карпат простягання, яке майже збігається із простяганням ототожненої площини розриву. Вісь стискання у механізмі вогнища спрямована на схід, що цілком узгоджується з північно-східним напрямком загальнорегіонального поля.

Ключові слова: повторні (схожі між собою) землетруси; кореляція хвильових форм; різницеві (диференційні) вступу; станційні поправки; механізм вогнища; розломно-блокова тектоніка; тектонічні напруження.

Received 31.08.2022